AJNR

Carotid Stent Delivery in an XMR Suite: Immediate Assessment of the Physiologic Impact of Extracranial Revascularization

Alastair J. Martin, David A. Saloner, Timothy P. L. Roberts, Heidi Roberts, Oliver M. Weber, William Dillon, Sean Cullen, Van Halbach, Christopher F. Dowd and Randall T. Higashida

AJNR Am J Neuroradiol 2005, 26 (3) 531-537
http://www.ajnr.org/content/26/3/531

Carotid Stent Delivery in an XMR Suite: Immediate Assessment of the Physiologic Impact of Extracranial Revascularization

Alastair J. Martin, David A. Saloner, Timothy P. L. Roberts, Heidi Roberts, Oliver M. Weber, William Dillon, Sean Cullen, Van Halbach, Christopher F. Dowd, and Randall T. Higashida

BACKGROUND AND PURPOSE: **Patients undergoing stent placement as treatment for severe stenosis of the internal carotid artery (ICA) were assessed with MR imaging in a combined MR–radiographic (XMR) angiography suite. MR imaging was performed before and immediately following conventional radiography–guided stent placement. Changes in MR imaging measurable properties, including flow and perfusion, resulting from stent placement were evaluated.**

PATIENTS AND TECHNIQUES: **MR imaging analysis was performed for 12 patients with >70% stenosis of the ICA before and after conventional radiography–guided deployment of a carotid stent. MR imaging acquisitions included angiography, quantitative flow analysis, perfusion, diffusion, and turbo–fluid-attenuated inversion recovery (FLAIR). These acquisitions were all performed immediately before and following stent placement by using conventional techniques.**

RESULTS: **MR angiography proved sufficient for identifying the target lesion and permitting targeted flow analysis. MR flow analysis demonstrated a marked increase in flow in the treated carotid artery (+2.2 ± 1.2 mL/s) and little change in other extracranial arteries. MR perfusion imaging showed no significant differences in relative cerebral blood volume between hemispheres before or after treatment, but there was a modest decrease in mean transit time and time to peak evident in the treated hemisphere after stent placement. Diffusion imaging did not demonstrate any ischemic foci resulting from carotid stent treatment. Hyperintensity of the CSF was noted on turbo-FLAIR acquisitions in the ipsilateral hemisphere following stent placement in 75% of patients.**

CONCLUSION: **MR imaging reliably reflects the state of the carotid artery and provides a means of monitoring and quantifying the effects of revascularization.**

A large body of evidence supports the use of intervention over medical therapy in symptomatic patients with an atherosclerotic stenosis of the carotid artery in the range of >50–70% in diameter (1–3). These large, multicenter studies have specifically demonstrated that surgical carotid endarterectomy reduces the incidence of ipsilateral strokes compared with medical therapy. Surgical endarterectomy, however, is invasive and is associated with morbidity and mortality that may vary by surgeon, institution, and experience (4). Accordingly, endovascular techniques are increasingly being used to treat carotid artery stenosis, especially in patients with high surgical risk or with failed carotid surgery due to restenosis (5). Endovascular techniques are less invasive, allow access to a larger portion of the carotid artery and do not require significant periods of transient vessel occlusion or bypass during treatment. Stent placement, rather than simple balloon angioplasty, achieves better intermediate and long-term results and is preferable to avoid the complications of vessel recoil and intimal dissection.

Carotid stent treatment is performed by using conventional radiographic techniques in an angiography suite. This is adequate for targeting regions of vessel narrowing and deployment of treatment aimed at restoring vessel patency. Conventional radiographic techniques do not, however, permit the quantitative

Received March 5, 2004; accepted after revision July 16.

From the Departments of Radiology (A.J.M., D.A.S., T.P.L.R., H.R., O.M.W., W.D., S.C., V.H., C.F.D., R.T.H.), Neurological Surgery (V.J., C.F.D., R.T.H.), and Neurology (V.H., C.F.D., R.T.H.), University of California—San Francisco, San Francisco, CA; and Philips Medical Systems (A.J.M.), Best, the Netherlands.

Address correspondence to Alastair J. Martin, PhD, University of California, San Francisco, Department of Radiology, Box 0628, Room L-310, 505 Parnassus Avenue, San Francisco, CA 94143.

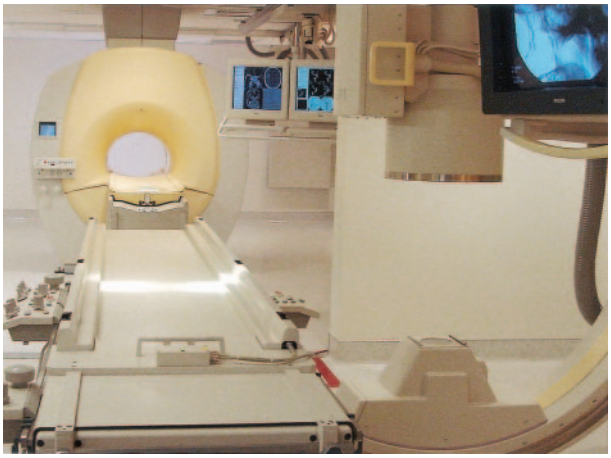

FIG 1. An XMR suite coupling an MR imaging scanner (*background*) with a catheterization lab (*foreground*). The patient lies on a floating tabletop that moves between the two systems on a continuous track. Magnetic isocenter and the conventional radiographic imaging position are separated by 6 m, and patients can be transferred between these two stations in less than 1 minute.

evaluation of arterial flow, tissue perfusion, or acute ischemic events. MR imaging offers these capabilities as well as being able to produce high-quality contrast-enhanced angiograms via a simple intravenous injection of contrast material. MR angiograms are increasingly being used to screen patients suspected of having vascular disease before cerebral digital subtraction angiography. MR imaging also permits quantification of flow changes, assessment of downstream tissue perfusion, and direct visualization of soft-tissue properties relevant to the treatment.

In this study, we assessed patients undergoing carotid artery stent placement for treatment of a stenosis of the cervical internal carotid artery. MR imaging was performed immediately before and immediately after stent placement under conventional radiographic guidance. MR-measurable physiologic changes resulting from stent placement were evaluated.

Patients and Techniques

All imaging was performed in a combined MR-conventional radiography (XMR) suite consisting of a short-bore 1.5T MR scanner (Philips Intera; Best, the Netherlands) and an integrated conventional radiographic catheterization laboratory (Philip Integris V5000). The two units were connected via a floating tabletop, permitting rapid patient transfer between the two systems (Fig 1). The MR imaging system was equipped with gradients capable of 30 mT/m amplitudes and 150 mT/m/ms slew rates and featured an in-room operator's console. A phased-array head/neck coil or a phased-array head-only coil was used for all patients. Because of coverage limitations, the latter was chosen only when prior imaging studies definitively demonstrated the lesion to be in the distal portion of the cervical internal carotid artery. The radio-frequency (RF) coil was removed following MR imaging and the patient was transported between the MR and conventional radiographic systems in a floating fashion via the MR tabletop. The radiographic system was single plane with a 15-inch image intensifier and was capable of 3D rotational angiography (3DRA).

Patients

Twelve patients scheduled to undergo placement of a stent as treatment for significant narrowing (>70%) of the internal carotid artery were studied. A complete neurologic history was obtained before treatment, and all patients signed an informed consent form that was approved by the university's committee on human research. Six patients were experiencing symptoms thought to be related to the ICA narrowing at the time of treatment. Four patients had experienced a stroke at some point in their past, but not within a 3-month period before stent placement. The catheterization procedure was performed under conscious sedation, whereas the MR examinations were performed immediately before and after the establishment of conscious sedation. Supplemental oxygen was administered during the catheterization procedure, but not during MR acquisitions. Patients ranged in age from 47 to 86 years (mean age, 65 years) and included six men and six women.

MR Acquisitions

MR imaging was performed immediately before and after endovascular treatment. MR acquisitions included contrast-enhanced MR angiography (CE-MRA; TR/TE/flip angle, 5 ms/1.65 ms/30°; FOV, 24 cm; rectangular FOV [rFOV], 70%; matrix, 320 × 240; sections, 70–0.75 mm; coronal plane; acquisition time, 36 seconds), diffusion-weighted imaging (TR/TE/flip angle, 3749 ms/81 ms/90°; epi factor, 77; *b*-value, 1000 s/mm^2; FOV, 24 cm; matrix, 128 × 77; sections, 24–5 mm; number of signal intensity averages [NSA], 3; axial plane; acquisition time, 48 seconds), postcontrast turbo–fluid-attenuated inversion recovery (FLAIR; TR/TE/TI/flip angle, 11000 ms/140 ms/2800 ms/90°; turbo factor, 47; FOV, 22 cm; rFOV, 75%; matrix, 256 × 179; sections, 30–5 mm; NSA, 2; axial plane; acquisition time, 3 minutes 18 seconds), phase contrast quantitative flow (Qflow; TR/TE/flip angle, 13 ms/7.9 ms/15°; FOV, 15 cm; rFOV, 70%; matrix, 128 × 128; sections, 1–5 mm; maximum velocity, 100 cm/s; number of heart phases, 15; NSA, 2; oblique plane; acquisition time, ~2.5 minutes, cardiac gated) and T2* perfusion (Perf; TR/TE/flip angle, 2000 ms/50 ms/90°; epi factor, 89; FOV, 24 cm; matrix, 128 × 89; sections, 12–5 mm; number of dynamics, 60; axial plane; acquisition time, 2 minutes 6 seconds). When the phased-array head coil was used, a SENSE factor of two was employed for CE-MRA, permitting 90 0.6-mm sections in 30 seconds (rFOV, 85%).

T1-shortening gadolinium-based contrast (Omniscan; Amersham Health, Princeton, NJ) for MR angiograms was administered at 2 mL/s to a total dose of 0.2 mmol/kg and was followed by a 15 mL saline push also at 2 mL/s. A fluoroscopic acquisition was used to trigger the start of the angiographic sequence following opacification of the proximal carotid arteries. DW imaging data were visually compared both pre- and poststent placement to determine whether any focal ischemic sequela occurred. Postcontrast turbo-FLAIR imaging was used to assess for possible subclinical ischemia and to detect any changes following stent treatment. Flow was quantified in both internal carotid arteries, as well as the vertebral or basilar arteries of the posterior cerebral circulation. A scan plane was selected just inferior or superior to the stenosis and was obliqued to be approximately perpendicular to the vessels. Because the Qflow measurement would be repeated following stent placement, the level was selected to be just outside the anticipated location of the stent and in a region of minimal vessel tortuosity. Perfusion data were fit to a standard gamma

TABLE 1: Patient summaries

Patient	Age	Stenosis Severity	Symptomatic	TFLR Enhancement
1	49	99	Yes	Strong
2	86	99	No	No
3	47	92	Yes	Slight
4	62	99	Yes	Slight
5	51	80	Yes	Slight
6	65	80	No	Strong
7	78	78	No	No
8	80	70	Yes	Strong
9	68	91	No	No
10	52	90	No	Strong
11	68	82	No	Slight
12	76	95	Yes	Slight

variate function, and the following parameters were extracted: relative cerebral blood volume (rCBV), mean transit time (MTT), time to arrival (T0), and time to peak (TTP). Gadolinium-based contrast (Omniscan) was administered at 4 mL/s to a dose of 0.2 mmol/kg and was followed by a 15-mL saline push also at 4 mL/s. The dynamics were set up to allow approximately 30 seconds of baseline imaging (no contrast) before the arrival of contrast and another 90 seconds of imaging following bolus arrival.

Angiography and Stent Placement Technique

Vascular access was obtained via a conventional femoral artery puncture, and preliminary diagnostic angiograms were performed in both carotid arteries and the dominant vertebral artery where appropriate. On the basis of these preliminary findings, the vessel to be treated was identified and the percent stenosis was determined by hand measurements. A targeted rotational angiogram was subsequently performed in the vessel to be treated. 3DRA was achieved via continuous conventional radiographic exposure and contrast (Omnipaque; Amersham Health) injection during a 180° sweep of the C-stand. A total of 120 projection images were acquired during this sweep, which takes 6 seconds. These data were reconstructed into a 3D volume and analyzed on an off-line workstation (Philips 3DRA Workstation). Stent placement was then performed following a previously defined technique (5). In this study, all patients received a nitinol self-expanding stent (Smart Stent or Precise Stent; Cordis Endovascular, Miami Lakes, FL). In 2/12 patients, the stent was deployed with a distal protection device in place (PercuSurge GuardWire; Medtronic, Santa Rosa, CA).

Results

All procedures were technical successes, and the stents were placed in the left carotid artery in five patients, the right carotid in six patients, and bilaterally in one patient (total, 13 stents). Stents were placed in arterial stenoses that were occluded between 70% and 99% of the normal lumen (mean, 88%) based on the North American Symptomatic Carotid Endarterectomy Trial criteria (1). Patient demographics are summarized in Table 1. All patients tolerated the procedure well, and no complications were noted in this cohort.

In all cases, the preliminary MR angiogram exhibited all relevant features of the internal carotid artery. Because of artifact following stent placement, posttreatment CE-MRA was performed in only one patient. Projection angiograms were obtained of all pertinent vessels, and these data were used for establishing percent stenosis and as roadmaps for stent delivery. Unlike conventional projection radiographic angiography, rotational reconstructions of the radiographic data had the benefit of producing volumetric data sets (similar to MR imaging) from which measurements could be made directly and manipulated in order to view in arbitrary orientations. This came at the expense of temporal information because of the 6-second rotation of the C-arm and with some penalty in the ability to delineate small vessels in the reconstructed data.

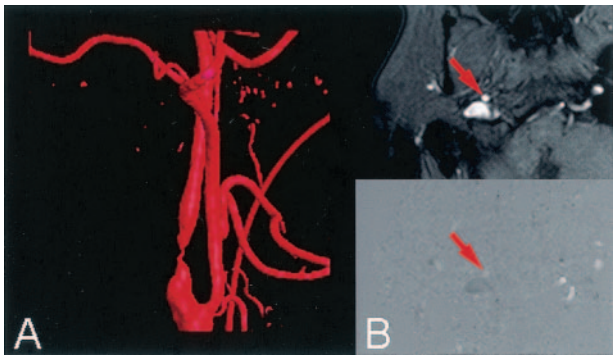

FIG 2. A very high-grade stenosis of the ICA depicted via 3DRA (*A*). Tight stenoses such as this could not be directly depicted with CE-MRA, although the presence of downstream contrast and measurable flow provide evidence of residual patency. *B,* Magnitude (*top*) and phase (*bottom*) MR images demonstrating the ICA (*arrows*) just distal to the stenosis, where the phase image reveals small, but nonzero, flow.

MR imaging was used to monitor flow changes (Fig 2), and this was successfully accomplished in all vessels before and following treatment. In 9/12 patients, it was possible to angulate a section to be essentially perpendicular to all vessels and thus accomplish flow analysis in one acquisition (Fig 3). In the remaining three patients, multiple Qflow acquisitions at varying scan plane obliquities were necessary to measure flow in both internal carotid arteries and the vertebral/basilar artery. Table 2 summarizes the changes in the stented internal carotid artery and compares these to other untreated vessels. The ipsilateral ICA category includes 13 vessels, whereas the contralateral ICA category contains only 11 vessels because one patient received bilateral stents. The listed error bars represent the standard deviation of measured blood flow across patients. A marked increase in blood flow in the stented vessel was present, which was most pronounced in highly stenotic and narrowed vessels. Vessels with a 95% or greater stenosis showed ipsilateral flow increases of $+3.0 \pm 1.0$ mL/s ($n = 4$), whereas stenoses between 70% and 80% produced a flow rate increase of $+1.2 \pm 1.0$ mL/s ($n = 4$). It is interesting to note that the contralateral and posterior cerebral circulation did not change significantly following placement of the stent. This implies cumulative flow has increased and that it may take a period of time to renormalize flow to the brain following vessel recanalization.

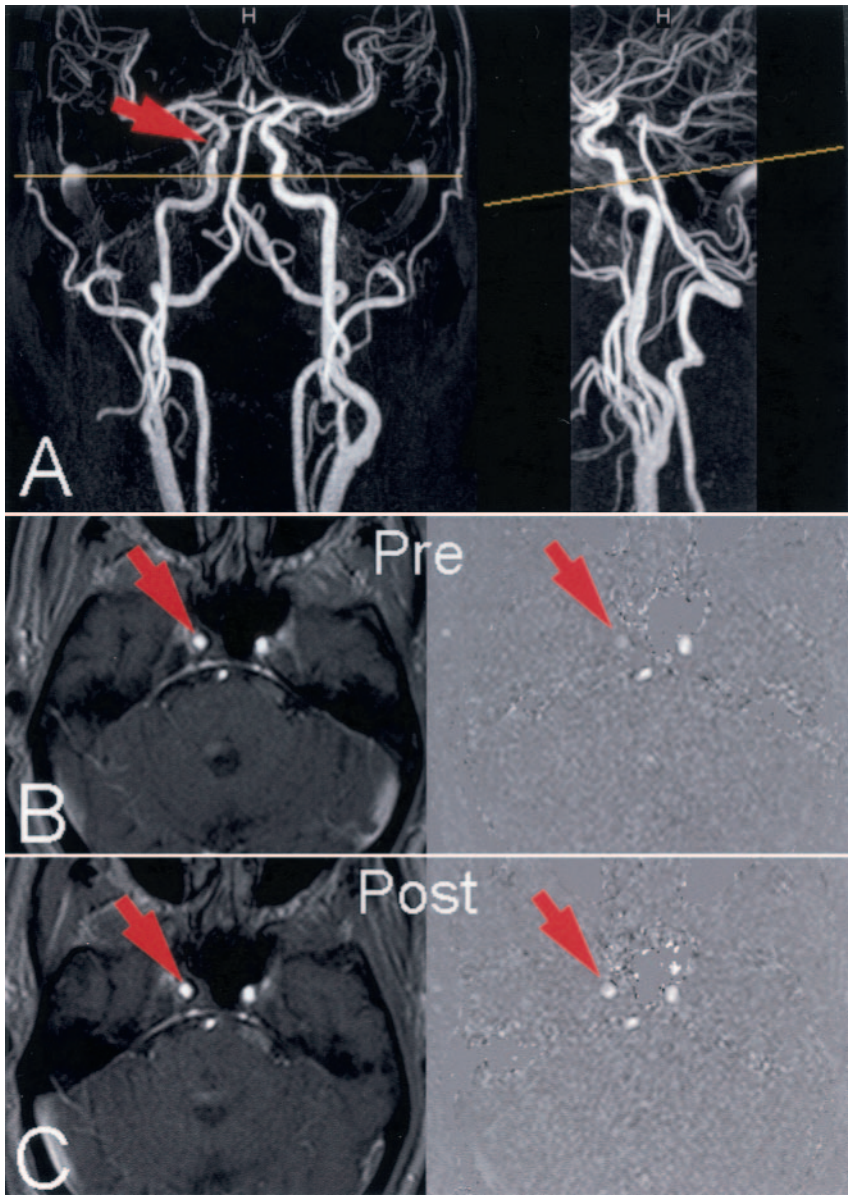

FIG 3. Measurement of flow changes within neck arteries is demonstrated. *A,* Section positioning (*line*) was performed on CE-MRA data such that the section was approximately perpendicular to the vessels and just distal or proximal to the stenosis (*arrow*). Qflow measurements were then performed at this site immediately before (*B*) and following (*C*) stent placement. Shown are the magnitude (*left*) and phase (*right*) images demonstrating the reproducibility of the scan plane and the increase in flow in the stented artery (*arrows*).

TABLE 2: Flow changes prior to and immediately following stent placement

Vessel	Flow − pre (mL/s)	Flow − post (mL/s)	Flow (mL/s)
Ipsilateral ICA	2.5 ± 1.2	4.7 ± 1.4	+2.2 ± 1.2
Contralateral ICA	4.7 ± 2.0	4.9 ± 2.1	+0.2 ± 0.8
Posterior circulation	3.3 ± 1.0	3.8 ± 1.6	+0.3 ± 0.9

Perfusion imaging failed to demonstrate focal regions of ischemia before stent placement in any of the patients in this study. In some cases, there were demonstrable differences in the timing maps of the ipsilateral hemisphere when compared with the contralateral hemisphere. These hemispheric differences typically resolved or even inverted following stent treatment (Fig 4). In addition, there were no new focal perfusion defects evident on the rCBV maps following stent placement. To assess global hemispheric changes over this patient population, we selected a section just superior to the lateral ventricles and compared the perfusion properties of each hemisphere before and after stent placement. This was accomplished by placing a region of interest over the entire hemisphere and averaging across all pixels within the region of interest. Table 3 summarizes these findings and demonstrates the relatively poor sensitivity of the technique to assess relatively subtle perfusion changes. A small bilateral increase in rCBV (+6%) following stent placement was noted, but this is much smaller than the variability we saw between the two measures (20% SD). Hemispheric differences in rCBV, pre- or poststent, similarly did not demon-

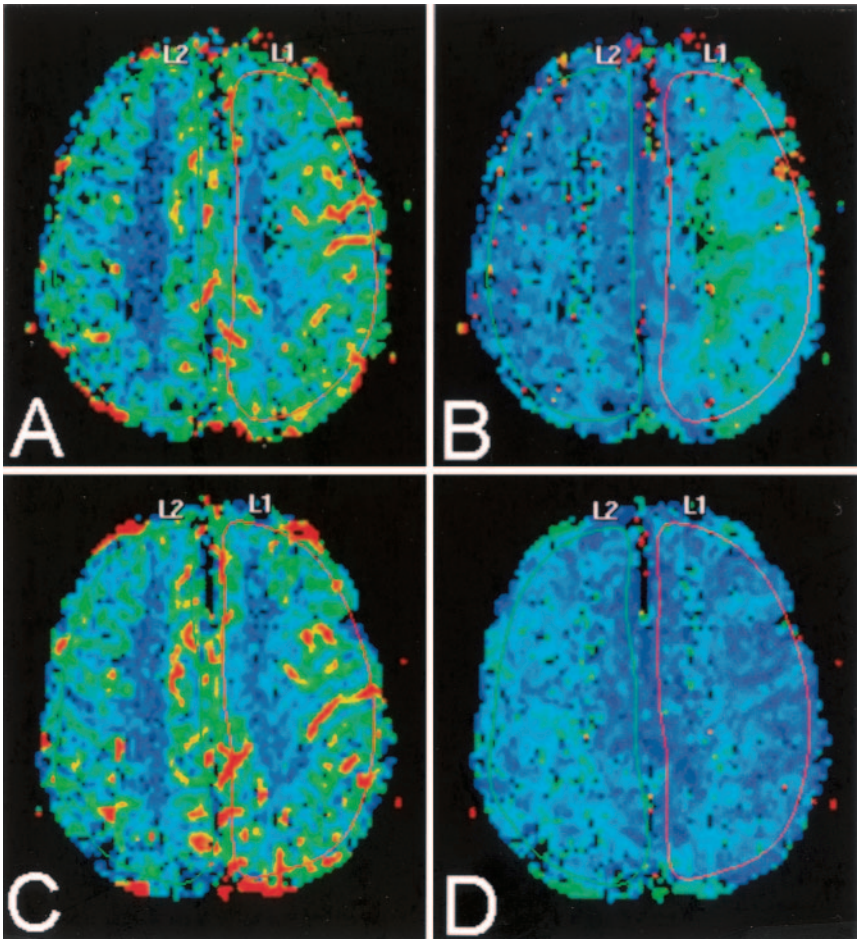

FIG 4. rCBV (*left column*) and TTP (*right column*) images obtained immediately before (*top row*) and following (*bottom row*) placement of a stent in the patient's left carotid artery. Initially the ipsilateral hemisphere exhibited delayed arrival times, but this reversed following treatment. The patient's contralateral ICA was also somewhat stenotic, and this may be responsible for the inversion following stent placement.

TABLE 3: Perfusion changes following stent placement

Hemisphere	CBV	MTT	T0	TTP
Ipsilateral	+6% ± 20%	−1.4 ± 1.1 s	+1.0 ± 1.1 s	−1.1 ± 1.5 s
Contralateral	+6% ± 17%	−0.6 ± 1.4 s	+0.4 ± 1.2 s	−0.3 ± 1.9 s

strate substantial or consistent differences in this subject group. The timing maps were somewhat more interesting, although none of the differences achieved statistical significance within this small sample group. A trend toward a slight shortening of the MTT and TTP in the ipsilateral hemisphere following stent placement was noted. This effect was less evident in the contralateral hemisphere, but again the variability across subjects was quite high.

The pre- and poststent diffusion images did not reveal any substantial differences. None of the patients had experienced a recent stroke before treatment and no clinically evident posttreatment ischemic complications were reported. The early time of these diffusion images, which were typically taken within 30 minutes of stent placement, may also hinder the detection of fresh focal ischemia resulting from dislodged emboli. Although no clinical evidence of such effects was noted, it remains possible that silent ischemia may have occurred without detection. Postcontrast turbo-FLAIR demonstrated high signal intensity within the ipsilateral CSF in portions of cerebral sulci in 75% of patients (Fig 5). This hyperintensity was in the CSF space of the ipsilateral cerebral sulci. It extended over the convexities of the ipsilateral hemisphere and included, but extended beyond, the watershed territory. This enhancement was evident only on posttreatment acquisitions and even appeared in one patient's poststent turbo-FLAIR acquisition that was accidentally run before the fresh administration of contrast. The implications of this assymmetry are currently not well understood and may arise either from leakage of the contrast agent (6) or possibly a change in the partial pressure of oxygen following recanalization (7).

Discussion

MR angiography consistently provided an accurate depiction of the location and extent of luminal narrowing of the internal carotid artery when compared with subsequent conventional radiographic angiograms. It is of some concern, however, that MR imaging techniques were less able to screen patients

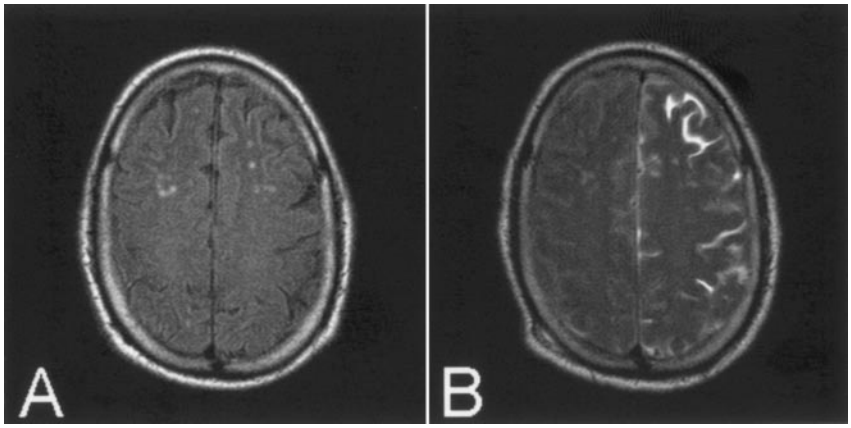

FIG 5. Turbo-FLAIR imaging performed before treatment (*left*) and immediately following (*right*) placement of a stent in the left carotid artery. Following treatment, substantial enhancement of the CSF is evident but spatially limited to the ipsilateral hemisphere. The pretreatment turbo-FLAIR was performed shortly after the administration of contrast but did not exhibit CSF enhancement.

following stent placement because of stent-related artifacts. Stents can produce artifacts in MR images due to either incompatibility of the magnetic susceptibility of the stent alloy or shielding of the RF energy emitted by the scanner (8). A nitinol-based stent was selected because of its MR imaging safety resulting from its relatively low magnetic susceptibility (9). RF attenuation within these carotid stents, however, remained problematic. It has previously been shown that the ability to visualize the lumen of even nitinol stents can vary widely (10, 11). It may be possible to improve visibility within the stent lumen by increasing the flip angle in the MRA protocol (12), but this is at the expense of signal intensity and contrast everywhere else in the imaging volume. A more appropriate solution is to alter the design of stents such that RF energy can more easily penetrate the device (13). This must be achieved, however, without compromising the structural properties of the stent, and doing so remains challenging with metallic alloys. The relative translucency of some stents in Maintz et al's (10) and Lenhart et al's (12) studies, however, does provide hope.

The demonstrated increase in blood flow following recanalization of a severely narrowed carotid artery seemed reasonable and also correlated with the severity of the stenosis before stent placement. It is perhaps more interesting to note that there was not an immediate reduction in flow in either the contralateral ICA or posterior circulation following stent placement. This implies that, at least in treated vessels with substantially flow-limiting stenoses, cumulative flow to the brain increases immediately following stent placement. In this study, we were not able to temporally monitor the patients over the following days to establish whether and when a redistribution of flow within the extracranial vessels would occur. In light of the fact that these patients were not exhibiting severe ischemia at the time of treatment, it would seem logical to expect that such a normalization of flow eventually would occur.

Monitoring perfusion changes with the existing first pass bolus techniques provided little insight into what, if any, changes where taking place in the perfusion bed. These MR perfusion techniques have shown the most promise in situations such as acute ischemic stroke, where severe ischemia may be present. It proved very difficult to demonstrate hemispheric differences in relative cerebral blood volume before treatment or a perceptible change in rCBV following treatment and recanalization. These findings are in agreement with a recently published study in a similar patient group (14). Because our patients were not exhibiting severe ischemia at the time of treatment, it can reasonably be suspected that any compromise in brain perfusion before stent placement would be subtle. Accordingly, we are not able to determine whether substantial perfusion changes following stent placement occurred or whether the technique simply lacks the sensitivity to detect the changes. Arterial spin labeling (15), which can quantify perfusion in mL/100 g/min may offer more hope. These techniques are currently being investigated; however, the use of spin labeling precludes any periprocedural use of MR imaging contrast material as this significantly alters the MR imaging properties of the blood for a prolonged period.

Diffusion-weighted images were routinely acquired primarily to determine whether hyperacute distal ischemia (16) could be detected. Our images showed no substantial changes between the pre- and poststent imaging sessions, and no clinically evident periprocedural strokes were reported in our patient cohort. Subclinical strokes associated with microemboli were also not detected, either because they did not exist or due to a lack of sensitivity of the diffusion images at this time scale. The hyperintensity of CSF on turbo-FLAIR acquisitions is somewhat more intriguing. This phenomenon was seen only on the ipsilateral hemisphere following stent placement and was primarily limited to the cortical convexities. The volume of conventional radiographic contrast did not correlate with the appearance of this pattern, because patients who did not demonstrate hyperintensity received similar radiographic contrast volumes (93 ± 38 mls administered ipsilaterally; 40 ± 6 mls to contralateral and posterior vessels) to those with slight (94 ± 27 mls administered ipsilaterally; 55 ± 10 mls to contralateral and posterior vessels) or strong enhancement (90 ± 36 mls administered ipsilaterally; 30 ± 2 mls to contralateral and posterior vessels). The treated artery, however, clearly does receive a substantially higher volume of radiographic contrast me-

dia. It remains possible, therefore, that a patient's preexisting vascular state made them susceptible to transient blood-brain barrier disruption during contrast administration. Leakage of residual gadolinium-based contrast from the preprocedural MR imaging study could then account for the CSF hyperintensity and provide some indication of the spatial distribution of the blood-brain barrier disruption.

Similar hyperintensity on turbo-FLAIR has been noted in patients undergoing balloon test occlusions of the carotid artery. Michel et al's study (6, pg 1590) attributed this hyperintensity to "pial or subarachnoid contrast staining in areas of altered perfusion without abnormalities on diffusion-weighted images." Although local leakage of contrast may be the cause of this phenomenon, it is also possible that changes in CSF oxygen tension might produce this effect. Hyperintensity of CSF has been noted on turbo-FLAIR images in patients breathing 100% oxygen, an effect that likely arises from altered CSF T1 (7). Although patients were not receiving supplemental oxygen during MR examinations, the altered blood flow pattern to the brain that was noted in this study could similarly have an effect on oxygen tension and produce a comparable result. This issue remains under active investigation.

Conclusion

MR imaging evaluation of carotid stent treatment demonstrated a significant increase in flow within the affected vessel, and this was most pronounced in highly stenotic vessels (>90%). Flow within the contralateral ICA and posterior circulation was not found to change substantially immediately following stent placement. First-pass bolus perfusion techniques demonstrated modest differences in contrast dynamics but could not demonstrate what perfusion changes, if any, occurred in the brain tissue. Similarly, the null result on diffusion imaging was consistent with no known embolic complications during stent deployment. The implications of ipsilateral enhancement on postcontrast turbo-FLAIR are currently under investigation.

References

1. North American Symptomatic Carotid Endarterectomy Trial Collaborators. **Beneficial effect of carotid endarterectomy in symptomatic patients with high-grade carotid stenosis: North American Symptomatic Carotid Endarterectomy Trial Collaborators**. *N Engl J Med* 1991;325:445–453
2. Barnett HJ, Taylor DW, Eliasziw M, et al. **Benefit of carotid endarterectomy in patients with symptomatic moderate or severe stenosis: North American Symptomatic Carotid Endarterectomy Trial Collaborators.** *N Engl J Med* 1998;339:1415–1425
3. Ferro JM, Oliveira V, Melo TP, et al. **Role of endarterectomy in the secondary prevention of cerebrovascular accidents: results of the European Carotid Surgery Trial (ECST).** *Acta Med Port* 1991;4:227–228
4. Halm EA, Chassin MR, Tuhrin S, et al. **Revisiting the appropriateness of carotid endarterectomy.** *Stroke* 2003;34:1464–1472
5. Phatouros CC, Higashida RT, Malek AM, et al. **Carotid artery stent placement for atherosclerotic disease: rationale, technique, and current status.** *Radiology* 2000;217:26–41
6. Michel E, Liu H, Remley KB, et al. **Perfusion MR neuroimaging in patients undergoing balloon test occlusion of the internal carotid artery.** *AJNR Am J Neuroradiol* 2001;22:1590–1596
7. Braga FT, da Rocha AJ, Hernandez G, et al. **Relationship between the concentration of supplemental oxygen and signal intensity of CSF depicted by fluid-attentuated inversion recovery imaging.** *AJNR Am J Neuroradiol* 2003;24:1863–1868
8. Klemm T, Duda S, Machann J, et al. **MR imaging in the presence of vascular stents: a systematic assessment of artifacts for various stent orientations, sequence types, and field strengths.** *J Magn Reson Imaging* 2000;12:606–615
9. Holton A, Walsh E, Anayiotos A, et al. **Comparative MRI compatibility of 316 L stainless steel alloy and nickel-titanium alloy stents.** *J Cardiovasc Magn Reson* 2002;4:423–430
10. Maintz D, Kugel H, Schellhammer F, Landwehr P. **In vitro evaluation of intravascular stent artifacts in three-dimensional MR angiography.** *Invest Radiol* 2000;36:218–224
11. Meyer JM, Buecker A, Spuentrup E, et al. **Improved in-stent magnetic resonance angiography with high flip angle excitation.** *Invest Radiol* 2001;36:677–681
12. Lenhart M, Volk M, Manke C, et al. **Stent appearance at contrast-enhanced MR angiography: in vitro examination with 14 stents.** *Radiology* 2000;217:173–178
13. Buecker A, Spuentrup E, Ruebben A, Gunther RW. **Artifact-free in-stent lumen visualization by standard magnetic resonance angiography using a new metallic magnetic resonance imaging stent.** *Circulation* 2002;105:1772–1775
14. Wilkinson ID, Griffiths PD, Hoggard N, et al. **Short-term changes in cerebral microhemodynamics after carotid stenting.** *AJNR Am J Neuroradiol* 2003;24:1501–1507
15. Detre JA, Leigh JS, Williams DS, Koretsky AP. **Perfusion imaging.** *Magn Reson Med* 1992;23:37–45
16. Wholey WM, Wholey M, Mathias K, et al. **Global experience in cervical carotid artery stent placement.** *Catheter Cardiovasc Interv* 2000;50:160–167